L_0 Smoothing Based Detail Enhancement for Fusion of Differently Exposed Images

Fei Kou*, Zhengguo Li†, Changyun Wen‡ and Weihai Chen*
* School of Automation Science and Electrical Engineering, Beihang University
Email: koufei@yeah.net, whchenbuaa@126.com
† Signal Processing Department, Institute for Infocomm Research
Email: ezgli@i2r.a-star.edu.sg
‡ School of Electrical and Electronic Engineering, Nanyang Technological University
Email: ecywen@ntu.edu.sg

***Abstract*—Exposure fusion is a technique to fuse several differently exposed low dynamic range (LDR) images to an LDR image. The output image has more information than each of the input images, but it could suffer from loss of fine details. In this paper, we propose a detail-enhanced exposure fusion algorithm by introducing an L_0 norm based optimization in gradient domain. The proposed algorithm extracts fine details from a vector field that is generated by using the gradient fields of the input images and adds the fine details to an intermediate image that is fused by an existing exposure fusion algorithm. Experimental results prove that the proposed method can enhance fine details for fused images.**

***Index Terms*—Exposure fusion, region of interest, detail-enhancement, gradient field, L_0 norm.**

I. INTRODUCTION

Most natural scenes have larger dynamic ranges than an image that a regular camera can record by a single shot. It makes images captured by the camera not the same as what humans see. This challenge was addressed by taking several differently exposed images for the same scene [1], [2]. In [2], Debevec et al. used multiple exposure images to synthesis a high dynamic range (HDR) image and then tone mapped the HDR image to an LDR image so as to display it on a conventional LDR display. To get more details in the final images, a lot of tone mapping algorithms were proposed to enhance the details, see for examples [3]–[6].

There is an alternative approach called exposure fusion [8]. The algorithms developed fuse a bracketed exposure sequence into a high quality image without generating a HDR image. In [8], Mertens et al. used a Laplacian decomposition of the images to fuse the images and a Gaussian pyramid to compute the weighted maps by considering the contrast, saturation and well-exposedness. Their scheme can merge images more quickly than the common HDR scheme. However, fine details could be missed in the result image. In [9], a detail enhanced exposure fusion scheme was proposed. Fine details are extracted from different images by solving a quadratic optimization problem in gradient domain, and then the details are added to an intermediate image fused by the exposure fusion scheme in [8]. The scheme in [9] is based on L_2 norm. It is shown experimentally in [6] that an L_0 norm based scheme could be adopted to produce better results. However, its computational cost is very high when fine details are extracted from a set of images, because as many optimization problems as the number of input images need to be solved by using the method. It is thus desirable to provide a new L_0 norm based detail-extraction method to extract details from a set of images.

In this paper, we propose a detail enhancement scheme for exposure fusion images. The major contributions is a novel fine detail extraction algorithm from a vector field. This is inspired by [9], while our algorithm is based on the L_0 norm. The proposed method is much simpler than the L_0 norm based method in [6] when fine details are extracted from a set of images and thus the computational cost is significantly reduced, because only one optimization problem needs to be solved. On the other hand, our experimental results prove the image generated by the proposed algorithm has as many fine details as the image generated with the input images detail-enhanced by the scheme in [6].

The remainder of this paper is organized as follows. In the next section, we introduce our detail-enhanced exposure fusion scheme. In Section III our experimental results are illustrated to verify the performance of our proposed schemes, and finally the paper is concluded in Section IV.

II. DETAIL-ENHANCED EXPOSURE FUSION

This section presents our detail-enhanced exposure fusion scheme. Our scheme first extracts fine details from all input images by solving an L_0 norm based optimization problem in gradient domain, and then adds the details to an image fused by the method in [8].

Firstly, we calculate the gradient fields of the image sequence. We denote the luma components of the input images as $Y_n(i,j)(1 \leq n \leq N)$. n is the index of the images. N is the number of all the input images - that is the number of the differently exposed images. The logarithmic conversion can measure local contrast by using spatial different [10], so we get the gradient in log domain. The gradient $\nabla \log(Y_n(i,j))(\partial_x \log(Y_n(i,j)), \partial_y \log(Y_n(i,j)))$ are defined as $(\log(Y_n(i,j+1)) - \log(Y_n(i,j)), \log(Y_n(i+1,j)) - \log(Y_n(i,j)))$. Basically, the image with the largest gradient among all the images records more details than the others. But the largest gradient image may be noisy. If we use the largest gradient directly, the noises are also enhanced. So we use a Gaussian low-pass filter to remove the noise. For the shape of the camera response function, the pixels which are almost white or black are less reliable than the well exposed pixels [2]. So the following weighting function is used:

$$W_n(i,j) = \begin{cases} Y_n(i,j)+1 & 0 \le Y_n(i,j) \le 127 \\ 256 - Y_n(i,j) & 128 \le Y_n(i,j) \le 255 \end{cases} \tag{1}$$

where $W_n(i,j)$ stands for the weight of the pixel (i,j) in the n-th image. A vector field computed by the weighted gradient field is given as

$$\begin{aligned} V_1(i,j) &= \max_{1\le n\le N}\{W_n(i,j)W_n(i,j+1)\frac{\partial \log(Y_n(i,j))}{\partial x}\} \\ V_2(i,j) &= \max_{1\le n\le N}\{W_n(i,j)W_n(i+1,j)\frac{\partial \log(Y_n(i,j))}{\partial y}\} \end{aligned} \tag{2}$$

Inspired by [6], we can get a objective funcion

$$\min_D \left\{ \lambda \cdot C(\partial_x D_p - V_{1,p}, \partial_y D_p - V_{2,p}) + \sum_p D_p^2 \right\} \tag{3}$$

where λ is a smoothing parameter, D is the value of the detail image. The subscript p denotes the p-th element of a vector or an image in this paper, For example, D_p is the p-th element of D. $C(\partial_x D_p - V_{1,p}, \partial_y D_p - V_{2,p}) = \#\{p \big| \, |\partial_x D_p - V_{1,p}| + |\partial_y D_p - V_{2,p}| \neq 0\}$, $\#$ stands for the number of p which satisfies $|\partial_x D_p - V_{1,p}| + |\partial_y D_p - V_{2,p}| \neq 0$, that is the L_0 norm.

There is a discrete counting metric in Eq. (3), it is thus very hard to solve. Same as [6], we introduce two auxiliary matrices h and v corresponding to $\partial_x D - V_1$ and $\partial_y D - V_2$ respectively to solve it. By solving the following optimization problem we can extract a detail image from the vector field (V_1, V_2)

$$\begin{aligned} \min_{D,h,v} \Bigg\{ \lambda \cdot C(h,v) + \sum_p \Big\{ D_p^2 + \beta\big((V_{1,p} - \partial_x D_p - h_p)^2 \\ + (V_{2,p} - \partial_y D_p - v_p)^2\big) \Big\} \Bigg\} \end{aligned} \tag{4}$$

where β is a parameter controls the similarity between h_p, v_p and $V_{1,p} - \partial_x D_p, V_{2,p} - \partial_y D_p$, h, v are auxiliary matrices to solve D. We can get when β is large enough, Eq. (4) and Eq.(origin) are equivalent. Similar to [6], the optimization problem (4) is solved through alternatively minimizing (h,v) and D. In each pass, one set of the variables are fixed with values obtained from the previous iteration. β is set as a small value β_0 at the beginning, and it is multiplied by κ each time, the calculation ends when β is larger than β_{max}. In our paper, β_0 has fixed value 2λ and β_0 has fixed value 10^5. The details are given as below.

Computing D when h and v are known: The D estimation subproblem corresponds to minimizing

$$\begin{aligned} \min_D \Bigg\{ \sum_p \Big\{ D_p^2 + \beta\big((V_{1,p} - \partial_x D_p - h_p)^2 \\ + (V_{2,p} - \partial_y D_p - v_p)^2\big) \Big\} \Bigg\} \end{aligned} \tag{5}$$

Similar to [6], the function has a global minimum, we accelerate the solver by diagonalizing derivative operators after Fast Fourier Transform (FFT). The solution is

$$D = -\mathscr{F}^{-1}\left(\frac{\beta(\mathscr{F}(\partial_x)\mathscr{F}(h - V_1) + \mathscr{F}(\partial_y)\mathscr{F}(v - V_2))}{\mathscr{F}(1) + \beta(\mathscr{F}(\partial_x)^*\mathscr{F}(\partial_x) + \mathscr{F}(\partial_y)^*\mathscr{F}(\partial_y))}\right) \tag{6}$$

where $\mathscr{F}$ is the FFT operator, $\mathscr{F}^{-1}$ is the IFFT operator and * denotes the complex conjugate.

Computing (h,v) when D is known: The objective function for (h,v) is

$$\begin{aligned} \min_{h,v} \Bigg\{ \sum_p \Big\{ (V_{1,p} - \partial_x D_p - h_p)^2 + (V_{2,p} - \partial_y D_p - v_p)^2 \Big\} \\ + \frac{\lambda}{\beta} C(h,v) \Bigg\} \end{aligned} \tag{7}$$

The solution is given by

$$(h_p, v_p) = \begin{cases} (0,0) & (V_{1,p} - \partial_x D_p)^2 + (V_{2,p} - \partial_y D_p)^2 \le \dfrac{\lambda}{\beta} \\ (V_{1,p} - \partial_x D_p, V_{2,p} - \partial_y D_p) & otherwise \end{cases} \tag{8}$$

By estimating D with equation (6) and h, v with equation (8) alternatively, and changing the value of β in every loop until it is larger than β_max, a detail image D can be extracted.

By using the exposure fusion method in [8], we can get an fused image. Let the luma component be denoted as Z_{fusion}, we can add the detail image to the fused image with the following equation

$$Z_{enhanced}(i,j) = Z_{fusion}(i,j) \cdot e^{D(i,j)} \tag{9}$$

Then a detail-enhanced exposure fusion image is obtained. The detail-enhanced image has more details than the fused image with the exposure fusion scheme in [8]. It is notable that our algorithm can be used to enhance all the exposure fusion schemes, we select the fusion scheme in [8] just because it is the most common exposure fusion scheme.

Now consider a special case that the vector field (V_1, V_2) is the gradient field of an image $I(i,j)$. By defining a new optimization variable $S(i,j)$ as $I(i,j) - D(i,j)$, we have the following optimization problem formulation:

$$\begin{aligned} \min_{S,h,v} \Bigg\{ \lambda \cdot C(h,v) + \sum_p \Big\{ (S_p - I_p)^2 + \beta\big((\partial_x S_p - h_p)^2 \\ + (\partial_y S_p - v_p)^2\big) \Big\} \Bigg\} \end{aligned} \tag{10}$$

which is exactly the problem formulated in [6]. This indicates that the optimization problem in [6] is a special case of our proposed optimization problem. Therefore our new formulation is applicable to extract details regardless of the number of input images. Note that when the method in [6] extracts details from a set of images, each image in the set needs to be decomposed once, whereas decomposition will be carried out once for the whole set of images when applying the proposed method here. Thus, the proposed algorithm is much simpler than that in [6] when details are extracted from a set of images, such as a set of differently exposed images in our paper. On the other hand, based on our experimental results, performance of the resulting image with our method is not sacrificed with the simplification.

III. Experimental results

(a) first input image (b) second input image (c) third input image

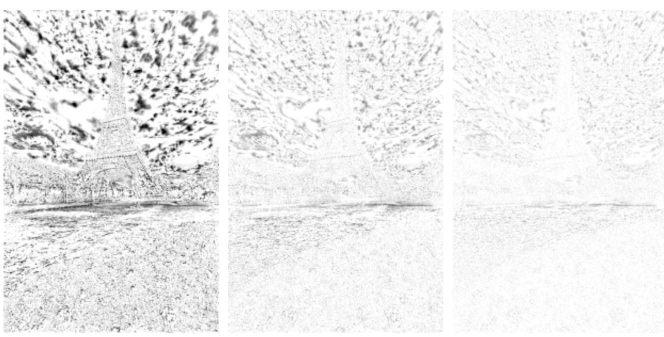

(d) extracted details by $\lambda = 0.02$ (e) extracted details by $\lambda = 0.005$ (f) extracted details by $\lambda = 0.002$

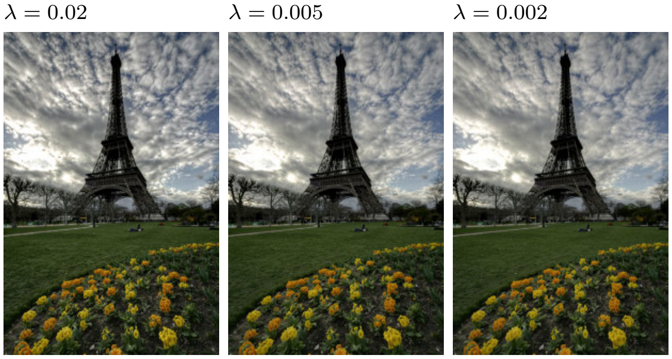

(g) detail-enhanced image by $\lambda = 0.02$ (h) detail-enhanced image by $\lambda = 0.005$ (i) detail-enhanced image by $\lambda = 0.002$

Fig. 1. Differently exposed input images and Comparison of different selections of λ. Image courtesy of Jacques Joffre.

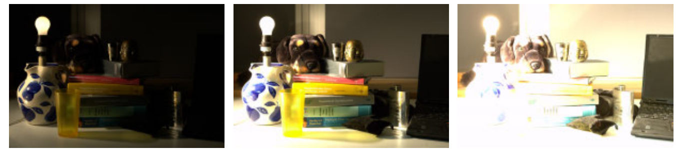

(a) first input image (b) second input image (c) third input image

(d) exposure fusion result (e) detail-enhanced image without a low-pass filter

(f) final image by the scheme in [9] (g) detail-enhanced image with a Gaussian low-pass filter

Fig. 2. Comparison of the different results with noisy input images in [11].

Readers are invited to read the paper by electronic version with full-size figures in order to better appreciate the differences among images. In this section, we first evaluate the choice of λ in (4). The images in Figs. 1 (a),1 (b),1 (c) are differently exposed images taken under the same lighting condition . Figs. 1(d), 1(e) and 1(f) are fine detail images extracted with different λ. By adding the fine details to the exposure fusion result in [8], Figs. 1(g), 1(h) and 1(i) are then obtained respectively. It can be shown that there are more details in these images than the exposure fusion result in Fig. 3(a), which is the exposure result of the images in Fig. 1 with the method in [8]. By comparing different selections of λ, we can draw a conclusion that a larger λ extracts more details and thus results in a sharper image. But an excessively large λ may result in over sharpened image.

We then study the generation of the vector field. The largest gradient is used to create the vector fields, but sometimes the maximum gradient is noisy. For example, the images in Figs. 2(a), 2(b) and 2(c) are taken with different exposure time at a large ISO value in [11]. The ISO value is too large so there are noises in the images. The detail-enhanced exposure fusion images without and with processing by a Gaussian low-pass filter are shown in Figs. 2(d) and 2(e), respectively. We can see Fig. 2(f) has more details than Fig. 2(d) but has less noise than Fig. 2(e). Clearly, the Gaussian low-pass filter can reduce the noises effectively.

As mentioned, the proposed method is much simpler than the method in [6] for exposure fusion image. Now the quality

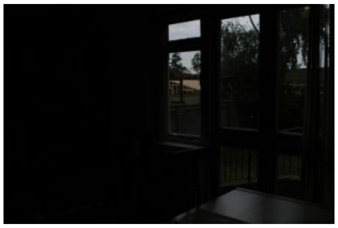

(a) first input image

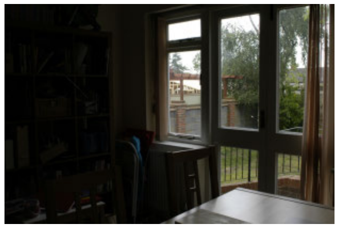

(b) second input image

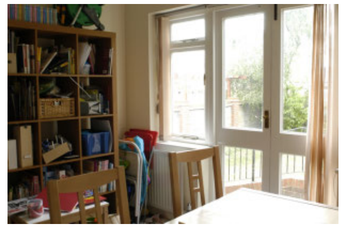

(c) third input image

(d) fourth input image

(e) final image by the scheme in [8]

(f) final image by the scheme in [9]

(g) final image by the proposed scheme

(h) fusion result with input images detail-enhanced by the scheme in [6]

Fig. 3. Differently exposed images in [8] and detail-enhanced exposure fusion results

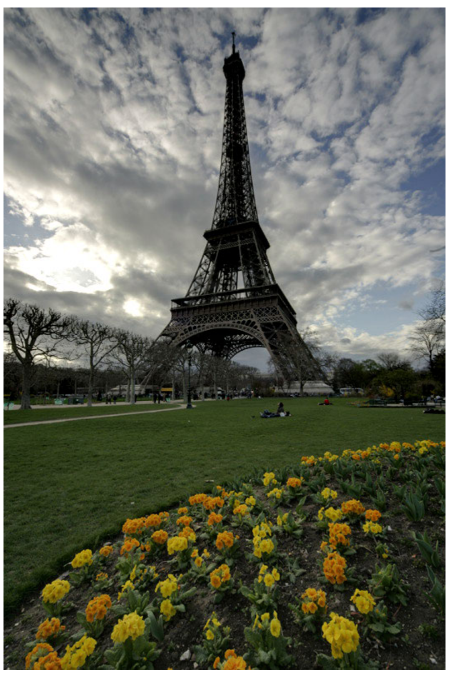

(a) Exposure fusion result by the scheme in [8]

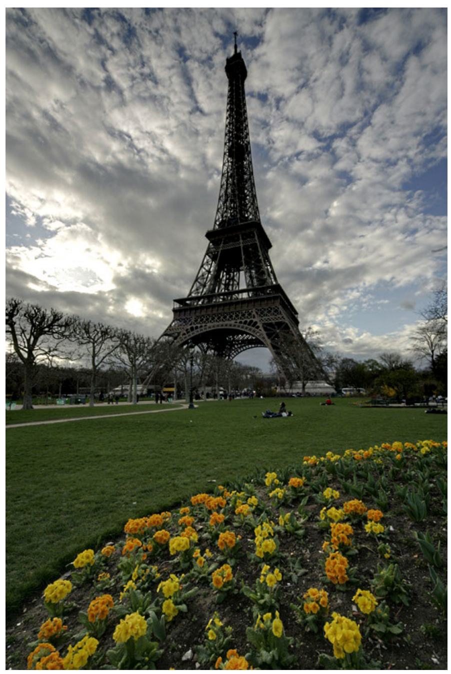

(b) Final image by the scheme in [9]

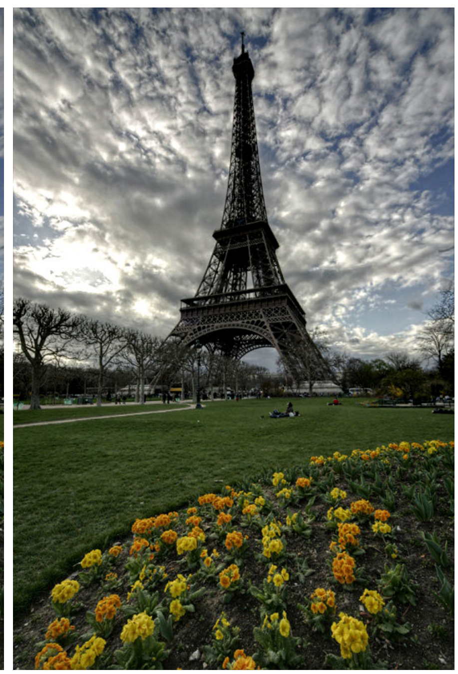

(c) Final image by the proposed scheme

Fig. 4. Detail-enhanced exposure fusion results of the images in Fig.1 .

of the images generated by the two methods is compared. The result image generated from the input images detail-enhanced with the scheme in [6] is shown in Fig. 3(d), while the image generated by our algorithm is given in Fig. 3(c), which shows more details. Additional sets of images are also tested and presented in Fig. 4, Fig. 5, Fig. 6 and Fig. 7. Based on all experimental results illustrated, our scheme can give more details than those in [6], [8], [9].

IV. Conclusion

In this paper, an L_0 norm based detail-enhancement scheme for exposure fusion images has been proposed. The proposed scheme is much simpler in enhancing details for exposure fusion images than the existing L_0 norm based scheme while quality is still maintained. The proposed scheme can extract the fine details from the differently exposed images simultaneously, and added them to an intermediate image that is fused by using an existing exposure fusion algorithm. As a result, the proposed scheme enhances the details of the exposure fusion

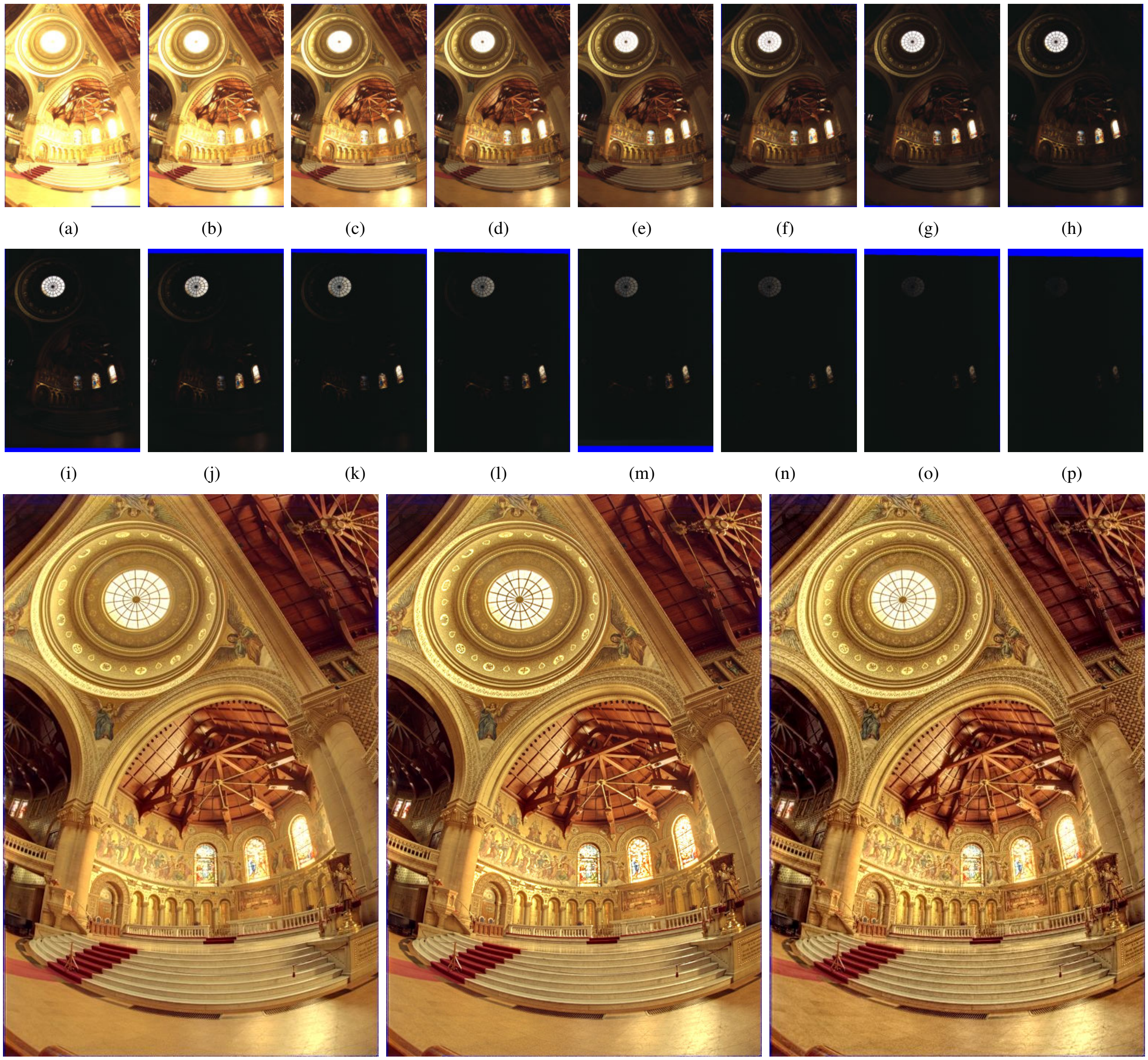

(a) (b) (c) (d) (e) (f) (g) (h)

(i) (j) (k) (l) (m) (n) (o) (p)

(q) Exposure fusion result by the scheme in [8]
(r) Final image by the scheme in [9]
(s) Final image by the proposed scheme

Fig. 5. Detail-enhanced exposure fusion results of the images in [2]. (a)-(p) are input images

image.

Acknowledgment

This work has been supported by National Nature Science Foundation of China under the research project 61075075 and 61175108.

References

[1] S. Mann and R. W. Picard, "On being 'undigital' with digital cameras: extending dynamic range by combining differently exposed pictures", *in Proc. of the 1995 IS&T's 48th Annual Conference*, pp. 442-448, 1995.

[2] P. E. Debevec and J. Malik, "Recovering high dynamic range radiance maps from photographs", *in Proc. of the 1997 Conference on Computer Graphics (SIGGRAPH)*, pp. 369-378, 1997.

[3] R. Fattal, D. Lischinshi, and M. Werman, "Gradient domain high dynamic range compression", *ACM Transactions on Graphics*, vol. 21, no. 3, pp. 6701-6710, 2002.

[4] F. Durand, and J. Dorsey, "Fast bilateral filtering for the display of high-dynamic-range images", *in Proc. of the 2002 Conference on Computer Graphics (SIGGRAPH)*, pp.257-265, 2002.

[5] Z. Farbman, R. Fattal, D. Lischinshi, and R. Szeliski, "Edge-preserving decompositions for multi-scale tone and details manipulation", *ACM Transactions on Graphics*, vol. 27, no. 3, pp.249-256, 2008.

[6] L. Xu, C. Lu, Y. Xu and J. Jia, "Image smoothing via L_0 gradient minimization", *ACM Transactions on Graphics (SIGGRAPH Asia 2011)*, vol. 30, no. 6, 2011.

[7] Z. G. Li, J. H. Zheng, and S. Rahardja, "Region-of-interest based local tone mappings," *In Proc. of the 6th IEEE Conference on Industrial Electronics and Applications*, pp.1547-1553, 2011.

[8] T. Mertens, J. Kautz, and F. Van Reeth, "Exposure fusion: A simple

(a) (b) (c) (d) (e) (f) (g) (h) (i)

(j) exposure fusion result by the scheme in [8] (k) final image by the scheme in [9] (l) final image by the proposed scheme

Fig. 6. Detail-enhanced exposure fusion results of the images in [3]. (a)-(i) are input images.

(a) first input image (b) second input image (c) third input image

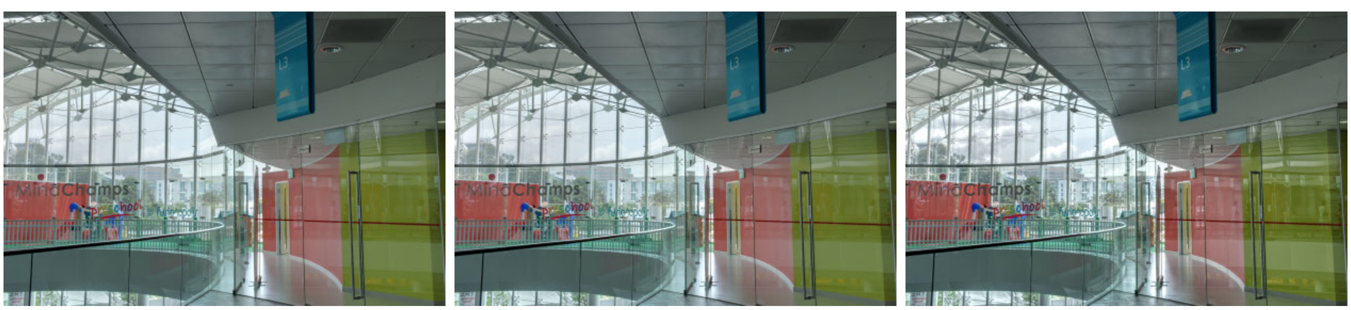

(d) Exposure fusion result by the scheme in [8] (e) Final image by the scheme in [9] (f) final image by the proposed scheme

Fig. 7. Detail-enhanced exposure fusion results of Fusionopolis.

and practical alternative to high dynamic range photography”, *Computer Graphics Forum*, vol. 28, no. 1, pp. 161-171, 2009.

[9] Z. G. Li, J. H. Zheng, and S. Rahardja, “Detail-enhanced exposure fusion”, *IEEE Transaction on Image Processing*, vol. 21, no. 11, pp. 4672-4676, 2012.

[10] R. Fattal, M. Agrawala, and S. Rusinkiewicz, “Multiscale shape and details enhancement for multi-light image collections,” *ACM Trans. Graphics*, vol. 26, no. 3, pp. 51:1C51:10, 2007.

[11] S. W. Hasinoff, F. Durand, and W. T. Freeman, “Noise-optimal capture for high dynamic range photography”, *in Proc. of 23rd IEEE Conference on Computer Vision and Pattern Recognition*, pp. 553-560, 2010